NATIONAL AERONAUTICS AND SPACE ADMINISTRATION

Technical Memorandum 33-364

A Criterion for Selecting Realistic Natural Modes of a Structure

W. C. Hurty

JET PROPULSION LABORATORY
CALIFORNIA INSTITUTE OF TECHNOLOGY
PASADENA, CALIFORNIA

November 1, 1967

NATIONAL AERONAUTICS AND SPACE ADMINISTRATION

Technical Memorandum 33-364

A Criterion for Selecting Realistic Natural Modes of a Structure

W. C. Hurty

Approved by:

W. H. Gayman, for

M. E. Alper, Manager
Applied Mechanics Section

JET PROPULSION LABORATORY
CALIFORNIA INSTITUTE OF TECHNOLOGY
PASADENA, CALIFORNIA

November 1, 1967

TECHNICAL MEMORANDUM 33-364

Prepared Under Contract No. NAS 7-100
National Aeronautics & Space Administration

Contents

Tables

Figures

Abstract

This document reports the development of a criterion to be used in determining the natural modes and frequencies of vibration of a structure by analysis of a suitable conceptual or mathematical model. Analyses of complex structures by the method of component mode syntheses typically yield results that are accurate in the lower modes and inaccurate in the higher modes. The equation developed in this report yields a criterion that indicates which modes are accurate, or representative of the real structure, and which modes are inaccurate. This criterion is applied to the analysis of a real structural system.

A Criterion for Selecting Realistic Natural Modes of a Structure

I. Introduction

All methods for vibration analysis of real structures are approximate methods, in the sense that the real structure (having in principle an infinite number of degrees of freedom) is represented by a model having a finite number. Analysis methods may be classified broadly under two categories: lumped parameter and modal methods. In lumped parameter methods, the physical aspect of the structure is altered in the modeling process by representing it as a finite number of rigid masses and massless, elastic connecting elements. In modal methods, the modeling process limits the virtual displacements of the structure to those that are defined by a finite number of assumed displacement modes. In either case, the effect of modeling is to introduce errors in the computed modes and frequencies of vibration. These errors are reduced generally by increasing the number of degrees of freedom *(dof)*, although a countereffect may be introduced by the possibility of increasing numerical round-off errors in the computations.

Nevertheless, it is common experience that an effective means of reducing errors and of gaining information concerning convergence of solutions is to improve the model in successive steps. This method requires several complete and independent solutions and is a laborious and time-consuming procedure.

The analysis carried out in this report represents an attempt to learn something about such errors by other means than carrying out successive solutions. It has been found that the results obtained lead to a useful criterion that enables the analyst to determine, within close limits, those natural modes resulting from the analysis of a particular model which closely represent natural modes of the actual structure as they might be illustrated by a greatly improved model.

II. Analysis

The ith natural mode and frequency of a structure are given by the following matrix equation:

$$\mathbf{M}\mathbf{q}_0^{(i)} = \lambda_{0_i} \mathbf{K}\mathbf{q}_0^{(i)} \tag{1}$$

where

$$\begin{aligned} \mathbf{M} &= \text{mass matrix} \\ \mathbf{K} &= \text{stiffness matrix} \\ \lambda_{0_i} &= i\text{th eigenvalue} \\ &= 1/\omega_{0_i}^2 \\ \omega_{0_i} &= \text{natural frequency in the } i\text{th mode} \\ \mathbf{q}_0^{(i)} &= \text{eigenvector in the } i\text{th mode} \end{aligned}$$

The subscript 0 denotes approximate results obtained by use of a conceptual model having a number of degrees of freedom appropriate to the needs of the problem at hand and the computer equipment available for the solution. The accuracy of the results can be bettered by an improvement in the conceptual model which generally results in a larger number of degrees of freedom. The eigenvalue problem associated with an improved model is written in Eq. (2), where it is assumed that the adopted coordinate system is one in which coupling occurs only in the mass matrix. An example is shown later in which such a coordinate system is illustrated.

$$\left[\begin{array}{c|c} M^{oo} & M^{on} \\ \hline M^{no} & M^{nn} \end{array}\right] \left\{\begin{array}{c} q^{o(i)} \\ \hline q^n \end{array}\right\} = \lambda_i \left[\begin{array}{c|c} K^{oo} & 0 \\ \hline 0 & K^{nn} \end{array}\right] \left\{\begin{array}{c} q^{o(i)} \\ \hline q^n \end{array}\right\} \tag{2}$$

where

$$\begin{aligned} M^{oo} &= \mathbf{M} = \text{mass matrix for the original model} \\ K^{oo} &= \mathbf{K} = \text{stiffness matrix for the original model} \\ M^{nn} &= \text{mass matrix associated with the added degrees of freedom in the improved model} \\ K^{nn} &= \text{stiffness matrix associated with the added degrees of freedom} \\ M^{on}, M^{no} &= \text{mass coupling matrices} \\ \lambda_i &= i\text{th eigenvalue for the improved model} \end{aligned}$$

and

$$\left\{\begin{array}{c} q^{o(i)} \\ q^n \end{array}\right\} = i\text{th eigenvector for the improved model}$$

Equation (2) can be written in two separate matrix equations as follows:

$$\mathbf{M}^{oo}\mathbf{q}^{o(i)} + \mathbf{M}^{on}\mathbf{q}^{n(i)} = \lambda_i \mathbf{K}^{oo}\mathbf{q}^{o(i)} \tag{3}$$

$$\mathbf{M}^{no}\mathbf{q}^{o(i)} + \mathbf{M}^{nn}\mathbf{q}^{n(i)} = \lambda_i \mathbf{K}^{nn}\mathbf{q}^{n(i)} \tag{4}$$

From Eq. (4), the subvector $\mathbf{q}^{n(i)}$ is found in terms of $\mathbf{q}^{o(i)}$ as follows:

$$\mathbf{q}^{n(i)} = (\lambda_i \mathbf{K}^{nn} - \mathbf{M}^{nn})^{-1} \mathbf{M}^{no}\mathbf{q}^{o(i)} \tag{5}$$

This is substituted into Eq. (3) to yield the following relationship:

$$[\mathbf{M}^{OO} + \mathbf{M}^{On} (\lambda_i \mathbf{K}^{nn} - \mathbf{M}^{nn})^{-1} \mathbf{M}^{nO}] \mathbf{q}^{n(i)} = \lambda_i \mathbf{K}^{OO} \mathbf{q}^{O(i)} \tag{6}$$

This equation expresses an eigenvalue problem of the same order as Eq. (1), from which improved eigenvalues and eigenvectors, λ_i and $\mathbf{q}^{O(i)}$, are expected. The original mass matrix is altered by the addition of an incremental mass matrix $\delta\mathbf{M}_i$, where

$$\delta\mathbf{M}_i = \mathbf{M}^{On} (\lambda_i \mathbf{K}^{nn} - \mathbf{M}^{nn})^{-1} \mathbf{M}^{nO} \tag{7}$$

Equation (6) may then be written in the form

$$(\mathbf{M} + \delta\mathbf{M}_i) \mathbf{q}^{O(i)} = \lambda_i \mathbf{K} \mathbf{q}^{O(i)} \tag{8}$$

It is noted that Eqs. (1) and (8) differ only by the addition of the incremental mass matrix $\delta\mathbf{M}_i$. Their solutions are compared by using the linear extrapolation

$$\lambda_i = \lambda_{0_{(i)}} + \delta\lambda_i \tag{9}$$

$$\mathbf{q}^{O(i)} = \mathbf{q}^{O(i)} + \delta\mathbf{q}^{(i)} \tag{10}$$

Substituting into Eq. (8) and subtracting Eq. (1) lead to the following result:

$$(\mathbf{M} - \lambda_{0_i} \mathbf{K})\, \delta\mathbf{q}^{(i)} + \delta\mathbf{M}_i \mathbf{q}_0^{(i)} + \delta\mathbf{M}_i \delta\mathbf{q}^{(i)} = \delta\lambda_i \mathbf{K} \mathbf{q}_0^{(i)} + \delta\lambda_i \mathbf{K} \delta\mathbf{q}^{(i)} \tag{11}$$

This equation is premultiplied by the transposed eigenvector in the jth mode $\mathbf{q}_0^{(j)T}$. The following scalar equation results:

$$\mathbf{q}_0^{(j)T} (\mathbf{M} - \lambda_{0_i} \mathbf{K})\, \delta\mathbf{q}^{(i)} + \mathbf{q}_0^{(j)T} \delta\mathbf{M}_i \mathbf{q}_0^{(i)} + \mathbf{q}_0^{(j)T} \delta\mathbf{M}_i \delta\mathbf{q}^{(i)} = \delta\lambda_i\, \mathbf{q}_0^{(j)T} \mathbf{K} \mathbf{q}_0^{(i)} + \delta\lambda_i\, \mathbf{q}_0^{(j)T} \mathbf{K} \delta\mathbf{q}^{(i)} \tag{12}$$

In case $j = i$, the first term in this equation vanishes by virtue of Eq. (1). If second-order terms are neglected, i.e.,

$$\left.\begin{aligned} \mathbf{q}_0^{(j)T} \delta\mathbf{M}_i \delta\mathbf{q}^{(i)} &= 0 \\ \delta\lambda_i \mathbf{q}_0^{(j)T} \mathbf{K} \delta\mathbf{q}^{(i)} &= 0 \end{aligned}\right\} \tag{13}$$

the following equation results:

$$\delta\lambda_i = \frac{\mathbf{q}_0^{(j)T} \delta\mathbf{M}_i \mathbf{q}_0^{(i)}}{\mathbf{q}_0^{(j)T} \mathbf{K} \mathbf{q}_0^{(i)}} \tag{14}$$

Using Eq. (1), this result can be expressed in the following form:

$$\frac{\delta\lambda_i}{\lambda_{0_i}} = \frac{\mathbf{q}_0^{(j)T} \delta\mathbf{M}_i \mathbf{q}_0^{(i)}}{\mathbf{q}_0^{(j)T} \mathbf{M} \mathbf{q}_0^{(i)}} \tag{15}$$

Either Eq. (14) or Eq. (15) can be used to estimate predicted improvements in the computed eigenvalue for any given mode brought about by the addition of new degrees of freedom associated with an improved conceptual model. It is emphasized that these results permit only an estimate of the correction because of errors introduced by neglecting the terms indicated in Eq. (13).

III. Application to the Method of Component Mode Synthesis

In the method of component mode synthesis (Refs. 1 and 2), Eq. (1) takes the following form.

$$\left[\begin{array}{c|c} M^{BB} & M^{BN} \\ \hline M^{NB} & M^{NN} \end{array}\right] \left\{\begin{array}{c} q_0^{B(i)} \\ \hline q_0^N \end{array}\right\} = \lambda_{0_i} \left[\begin{array}{c|c} K^{BB} & 0 \\ \hline 0 & K^{NN} \end{array}\right] \left\{\begin{array}{c} q_0^{B(i)} \\ \hline q_0^N \end{array}\right\} \tag{16}$$

In this equation, the superscript B relates to a set of basic coordinates that define two classes of generalized displacements of a structural system composed of a finite number of connected components. One class of displacements includes those in which the components undergo rigid-body displacements. The other class includes those that are compatible with generalized displacements of the redundant constraints in the connection system among the components. From another point of view, it can be said that the basic displacements are defined by (and are compatible with) displacements of the connection system. Because the number of connections is considered to be finite, it follows that $\{q_0^B\}$ is necessarily finite.

The superscript N in Eq. (16) relates to a set of normal coordinates that define displacements of the system relative to the connection system. It is convenient, although not necessary, to think of these coordinates as the normal coordinates of the components that define their vibration modes with all connections completely fixed. In this case, the submatrices $\mathbf{M}^{NN}$ and $\mathbf{K}^{NN}$ are diagonal. In any case, it is shown (Refs. 1 and 2) that the submatrices $\mathbf{K}^{BN}$ and $\mathbf{K}^{NB}$ are null matrices so long as the so-called normal coordinates define displacements relative to the connection system. It is clear that there is no limit to the number of normal coordinates so that $\{q_0^N\}$ is made finite only by selecting an arbitrary finite number of them. In terms of modal coordinates, one usually would begin with the lowest frequency modes and select as many modes, in the order of ascending mode numbers, as considered necessary.

The superscript n in Eq. (2) refers to an additional set of normal coordinates corresponding to higher modes beyond those selected for the original solution of Eq. (1).

The mass matrix in Eq. (2) may now be written as follows:

$$\left[\begin{array}{c|c} M^{OO} & M^{On} \\ \hline M^{nO} & M^{nn} \end{array}\right] = \left[\begin{array}{c|c|c} M^{BB} & M^{BN} & M^{Bn} \\ \hline M^{NB} & M^{NN} & 0 \\ \hline M^{nB} & 0 & M^{nn} \end{array}\right] \tag{17}$$

The two null submatrices clearly result from the choice of orthogonal normal modes. Similarly, the stiffness matrix has the form

$$\left[\begin{array}{c|c} K^{OO} & 0 \\ \hline 0 & K^{nn} \end{array}\right] = \left[\begin{array}{c|c|c} K^{BB} & 0 & 0 \\ \hline 0 & K^{NN} & 0 \\ \hline 0 & 0 & K^{nn} \end{array}\right] \tag{18}$$

The incremental mass matrix $\delta\mathbf{M}_i$ given by Eq. (7) may now be expressed as follows:

$$\delta\mathbf{M}_i = \left[\begin{array}{c} M^{Bn} \\ \hline 0 \end{array}\right] (\lambda_i K^{nn} - M^{nn})^{-1} \left[\begin{array}{c|c} M^{nB} & 0 \end{array}\right] = \left[\begin{array}{c|c} \delta M_i^{BB} & 0 \\ \hline 0 & 0 \end{array}\right] \tag{19}$$

where

$$\delta\mathbf{M}_i^{BB} = \mathbf{M}^{Bn} (\lambda_i \mathbf{K}^{nn} - \mathbf{M}^{nn})^{-1} \mathbf{M}^{nB} \tag{20}$$

The numerator on the right side of Eqs. (14) and (15) becomes

$$\mathbf{q}_0^{(i)T}\delta\mathbf{M}_i\mathbf{q}_0^{(i)} = \begin{Bmatrix} q_0^{B(i)} \\ \hline q_0^N \end{Bmatrix}^T \left[\begin{array}{c|c} \delta\mathbf{M}_i^{BB} & 0 \\ \hline 0 & 0 \end{array}\right] \begin{Bmatrix} q_0^{B(i)} \\ \hline q_0^N \end{Bmatrix}$$

$$= \quad q_0^{B(i)T}\,\delta\mathbf{M}_i^{BB}\,\mathbf{q}_0^{B(i)} \tag{21}$$

$$= \mathbf{q}_0^{B(i)T}\mathbf{M}^{Bn}\,(\lambda_i\mathbf{K}^{nn} - \mathbf{M}^{nn})^{-1}\,\mathbf{M}^{nB}\,\mathbf{q}_0^{B(i)}$$

The denominator on the right side of Eq. (14) may be rewritten in a similar way, as follows:

$$\mathbf{q}_0^{(i)T}\mathbf{K}\mathbf{q}_0^{(i)} = \begin{Bmatrix} q_0^{B(i)T} \\ \hline q_0^N \end{Bmatrix} \left[\begin{array}{c|c} K^{BB} & 0 \\ \hline 0 & K^{NN} \end{array}\right] \begin{Bmatrix} q_0^{B(i)} \\ \hline q_0^N \end{Bmatrix}$$

$$= \mathbf{q}_0^{(i)BT}\mathbf{K}^{BB}\mathbf{q}_0^{(i)B} + \mathbf{q}_0^{(i)NT}\mathbf{K}^{NN}\mathbf{q}_0^{(i)N} \tag{22}$$

From Eq. (16) it is seen that $\mathbf{q}_0^{(i)N}$ can be expressed in terms of $\mathbf{q}_0^{(i)B}$, as follows:

$$\mathbf{q}_0^{(i)N} = -\,(\mathbf{M}^{NN} - \lambda_{0_i}\mathbf{K}^{NN})^{-1}\,\mathbf{M}^{NB}\mathbf{q}_0^{(i)B} \tag{23}$$

Substituting this into Eq. (22) yields the following:

$$\mathbf{q}_0^{(i)T}\mathbf{K}\mathbf{q}_0^{(i)} = \mathbf{q}_0^{(i)BT}\,[\mathbf{K}^{BB} + \mathbf{M}^{BN}\,(\mathbf{M}^{NN} - \lambda_{0_i}\mathbf{K}^{NN})^{-1}\,\mathbf{K}^{NN}\,(\mathbf{M}^{NN} - \lambda_{0_i}\mathbf{K}^{NN})^{-1}\,\mathbf{M}^{NB}]\;\mathbf{q}_0^{(i)B} \tag{24}$$

Hence, Eq. (14) may take the form

$$\delta\lambda_i = \frac{\mathbf{q}_0^{(i)BT}\,\mathbf{M}^{Bn}\,(\lambda_i\mathbf{K}^{nn} - \mathbf{M}^{nn})^{-1}\,\mathbf{M}^{nB}\mathbf{q}_0^{(i)B}}{\mathbf{q}_0^{(i)BT}\,[\mathbf{K}^{BB} + \mathbf{M}^{BN}\,(\mathbf{M}^{NN} - \lambda_{0_i}\mathbf{K}^{NN})^{-1}\,\mathbf{K}^{NN}\,(\mathbf{M}^{NN} - \lambda_{0_i}\mathbf{K}^{NN})^{-1}\,\mathbf{M}^{NB}]\;\mathbf{q}_0^{(i)B}} \tag{25}$$

As it stands, this equation must be solved by iteration, using Eq. (9), because the eigenvalue λ_i, appearing in the numerator on the right side, is unknown. Hence, it will be more convenient to simplify the equation by substitution of Eq. (9) directly, although this procedure involves an additional approximation. Attention is focused on the matrix $\lambda_i\mathbf{K}^{nn} - \mathbf{M}^{nn}$, which is a diagonal matrix in which the jth diagonal element is $\lambda_i\mathbf{K}_j^{nn} - \mathbf{M}_j^{nn}$. Note that

$$\mathbf{K}_j^{nn} = \frac{1}{\lambda_{n_j}}\,\mathbf{M}_j^{nn}$$

where

$$\lambda_{n_j} = \frac{1}{\omega_{n_j}^2}$$

and ω_{n_j} is a natural frequency of the appropriate component with fixed constraints. Therefore,

$$\lambda_i\mathbf{K}_j^{nn} - \mathbf{M}_j^{nn} = \frac{\lambda_i - \lambda_{n_j}}{\lambda_{n_j}}\,\mathbf{M}_j^{nn}$$

The jth element of the inverse matrix $(\lambda_i \mathbf{K}^{nn} - \mathbf{M}^{nn})^{-1}$ is $\dfrac{\lambda_{n_j}}{\lambda_i - \lambda_{n_j}} \mathbf{M}_j^{nn^{-1}}$

If Eq. (9) is substituted, the above fraction can be expanded in a power series in $\delta\lambda_i$, thus,

$$\frac{\lambda_{n_j}}{\lambda_i - \lambda_{n_j}} = \frac{\lambda_{n_j}}{\lambda_{0_i} - \lambda_{n_j}} - \frac{\lambda_{n_j}}{(\lambda_{0_i} - \lambda_{n_j})^2}\delta\lambda_i + \text{higher order terms in } \delta\lambda_i$$

The inverse matrix may be written, neglecting the higher-order terms, as follows:

$$(\lambda_i \mathbf{K}^{nn} - \mathbf{M}^{nn})^{-1} = \mathbf{H}\mathbf{M}^{nn^{-1}} - \mathbf{L}_n \mathbf{M}^{nn^{-1}} \delta\lambda_i$$

where

$$\mathbf{H} = \left[\diagdown \frac{\lambda_n}{\lambda_{0_i} - \lambda_n} \diagdown\right] \qquad \text{a diagonal matrix}$$

$$\mathbf{L}_n = \left[\diagdown \frac{\lambda_n}{(\lambda_{0_i} - \lambda_n)^2} \diagdown\right] \qquad \text{a diagonal matrix}$$

In a similar way, the denominator on the right side of Eq. (25) can be reduced, as follows:

$$(\mathbf{M}^{NN} - \lambda_{0_i}\mathbf{K}^{NN})^{-1}\mathbf{K}^{NN}(\mathbf{M}^{NN} - \lambda_{0_i}\mathbf{K}^{NN})^{-1} = \mathbf{L}_N \mathbf{M}^{NN^{-1}}$$

where

$$\mathbf{L}_N = \left[\diagdown \frac{\lambda_N}{(\lambda_{0_i} - \lambda_N)^2} \diagdown\right] \qquad \text{a diagonal matrix}$$

When the foregoing expressions are substituted into Eq. (25) that equation takes the following form:

$$\delta\lambda_i = \frac{\mathbf{q}_0^{(i)B^T}\mathbf{M}^{Bn}\mathbf{H}\mathbf{M}^{nn^{-1}}\mathbf{M}^{nB}\mathbf{q}_0^{(i)B}}{\mathbf{q}_0^{(i)B^T}[\mathbf{K}^{BB} + \mathbf{M}^{BN}\mathbf{L}_N\mathbf{M}^{NN^{-1}}\mathbf{M}^{NB} + \mathbf{M}^{Bn}\mathbf{L}_n\mathbf{M}^{nn^{-1}}\mathbf{M}^{nB}]\,\mathbf{q}_0^{(i)B}} \tag{26}$$

This equation may be expressed in summation form for computational purposes, as follows:

$$\delta\lambda_i = \frac{\displaystyle\sum_{j=1}^{n_B}\sum_{k=1}^{n_B} q_{0_j}^{(i)B} q_{0_k}^{(i)B} \sum_{l=n_T+1}^{n_T+n_A} \frac{M_{jl}^{BN}M_{kl}^{BN}}{M_{ll}^{NN}} \cdot \frac{\lambda_{N_l}}{\lambda_{0_l} - \lambda_{N_l}}}{\displaystyle\sum_{j=1}^{n_B}\sum_{k=1}^{n_B} q_{0_j}^{(i)B} q_{0_k}^{(i)B} \left\{K_{jk}^{BB} + \sum_{l=n_B+1}^{n_T+n_A} \frac{M_{jl}^{BN}M_{kl}^{BN}}{M_{ll}^{NN}} \cdot \frac{\lambda_{N_l}}{(\lambda_{0_l} - \lambda_{N_l})^2}\right\}} \tag{27}$$

where

n_B = number of basic degrees of freedom of the system

n_T = total number of degrees of freedom of system whose eigenvalues and eigenvectors are λ_{0_i}, $\mathbf{q}_0^{(i)}$, respectively.

n_A = number of additional fixed-constraint normal modes chosen to represent the true system.

In using Eq. (27) a set of eigenvalues, λ_{0_i}, and eigenvectors, $q_0^{(i)}$ will have been obtained from a solution of the system having n_T *dof* of which n_B represents the number of basic *dof*. To carry out these solutions, elements of the stiffness matrix K^{BB} and those of the mass matrices M^{BN}, M^{NN}, up to n_T degrees of freedom will have been obtained. In addition, masses corresponding to the added *dof* n_A must be determined as well as the additional quantities λ_N.

In principle, if an exact solution is to be obtained for purposes of comparison $n_A \to \infty$. However, it will be found that this number may remain finite because $\delta\lambda \to 0$ as n_A is increased. In practice, a limit will be reached beyond which further added degrees of freedom will have no substantial effect on the results.

IV. An Example

The foregoing procedure is applied to the structure shown in Fig. 1. It is a plane frame composed of uniform beams of various cross-sections connected rigidly together. All beams are considered to be axially rigid. The base of the central beam is fixed rigidly to ground. The in-plane natural modes and frequencies of this structure have been determined by using the method of component mode synthesis (Refs. 1 and 2). Results were obtained using six different generalized coordinate systems having 16, 24, 32, 40, 48, and 56 *dof*. The structure has eight basic *dof* indicated by the eight basic displacement coordinates shown in Fig. 2. For the 16-*dof* model, the first of the fixed-fixed normal modes of each of the eight members, identified by the numbered sectional views in Fig. 1, are included. Note that all members are fixed at both ends except No. 2, which is a cantilever. The 24-*dof* model includes the first two fixed-fixed normal modes of each member. The remaining models are obtained by adding up the third through the sixth normal modes of each member.

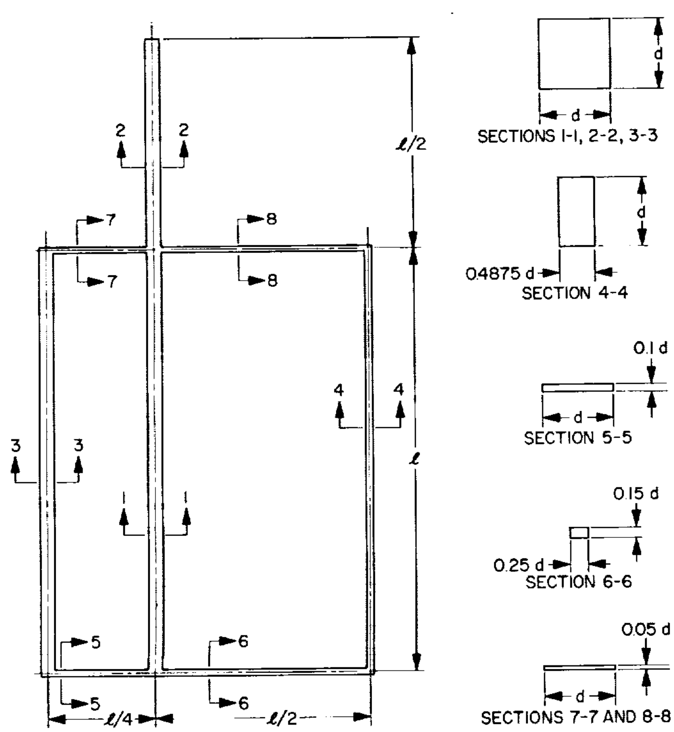

Figure 1. Frame structure treated in example

The complete sets of eigenvalues and eigenvectors for each of the six models are available but not reported in this paper. Only those having a significant bearing on the results of this study are given. In Table 1, the mode numbers related to each model are listed in the order of

Table 1. Comparison of mode numbers

Type of Mode	16 dof	24 dof	32 dof	40 dof	48 dof	56 dof
G	1	1	1	1	1	1
G	2	2	2	2	2	2
G	3	3	3	3	3	3
L	4	4	4	4	4	4
G	5	5	5	5	5	5
G	6	6	6	6	6	6
G	7	7	7	7	7	7
L	—	8	8	8	8	8
L	8	9	9	9	9	9
L	9	10	10	10	10	10
G	10	11	11	11	11	11
L	—	—	12	12	12	12
G	11	12	13	13	13	13
L	12	13	14	14	14	14
L	—	14	15	15	15	15
L	—	—	—	16	16	16
G	13	15	16	17	17	17
G	14	17	17	18	18	18
L	—	16	18	19	19	19
G	—	18	19	20	20	20
L	—	—	—	—	21	21
L	—	—	20	21	22	22
G	—	19	21	22	23	23
L	—	—	—	—	—	24
G	—	—	22	23	24	25
G	—	—	—	24	25	26
L	—	—	23	25	26	27
L	—	—	24	26	27	28
G	—	—	—	27	28	29
L	—	—	—	28	29	30
G	—	—	—	30	30	31
L	—	—	—	29	31	32
G	—	—	—	31	32	33

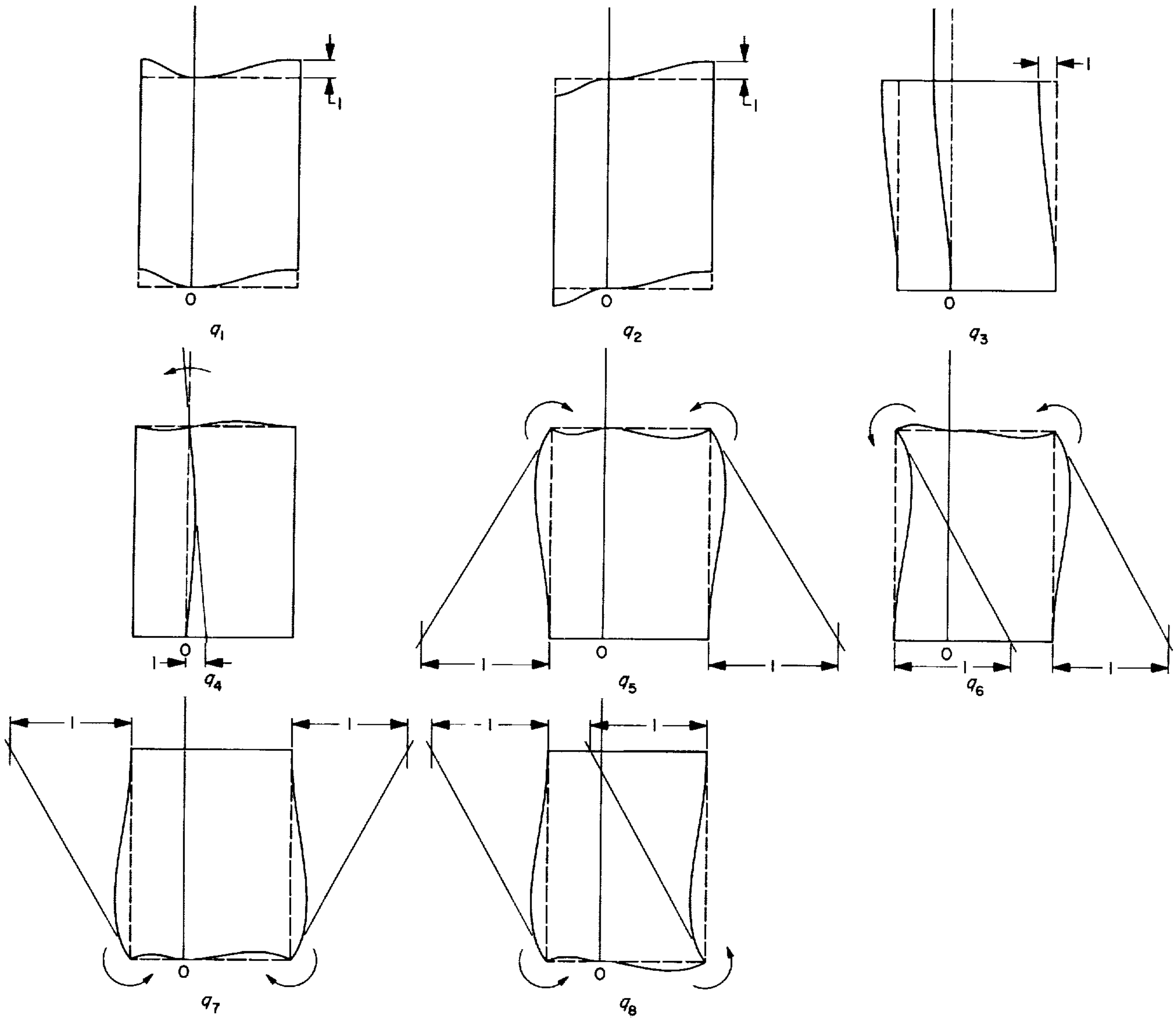

Figure 2. Generalized basic displacement coordinates

descending eigenvalues, or ascending frequencies. This table shows that a given mode does not necessarily carry the same mode number horizontally across the table; i.e., it may have a different position in the frequency spectrum related to the different models. The reason for this is that the introduction of new displacement coordinates associated with the fixed-fixed normal modes of some of the members gives rise to localized eigenmodes in which the primary response is associated with those particular members. Thus, the system eigenvalues associated with those localized modes are very nearly equal to the eigenvalues for the corresponding fixed-fixed modes. The members that contribute to this behavior are Nos. 5, 6, 7, and 8, which are quite flexible as compared with other members to which they connect; therefore, they may vibrate locally in modes that approximate very closely their own fixed-fixed modes. The first six fixed-fixed eigenvalues for all members of the system are listed in Table 2. The localized modes are identified in Table 1 by the letter *L*. In contrast, the *G*, or general, modes are those in which the entire system responds, as indicated by eigenfrequencies distinct from the local member frequencies and by sizable response in the q_0^B, or basic, part of the eigenvectors. It is the system behavior in these latter modes that is of concern in this report. Table 1 does not include a comparison of the higher mode numbers because a casual examination of the modal frequencies and vectors beyond the numbers listed shows a complete

Table 2. Fixed- constraint eigenvalues of members

Member	Mode 1	Mode 2	Mode 3	Mode 4	Mode 5	Mode 6
1	0.19977469 E-02	0.26291317 E-03	0.68410542 E-04	0.25035174 E-04	0.11218886 E-04	0.57510490 E-05
2	0.50556673 E-02	0.12872827 E-03	0.16419083 E-04	0.42757627 E-05	0.15646972 E-05	0.70118040 E-06
3	0.19977469 E-02	0.26291317 E-03	0.68410542 E-04	0.25035174 E-04	0.11218886 E-04	0.57510490 E-05
4	0.84060359 E-02	0.11062750 E-02	0.28785499 E-03	0.10534194 E-03	0.47206361 E-04	0.24199023 E-04
5	0.78036988 E-03	0.10270045 E-03	0.26722868 E-04	0.97793657 E-05	0.43823775 E-05	0.22465036 E-05
6	0.55492975 E-02	0.73031423 E-03	0.19002928 E-03	0.69542164 E-04	0.31163573 E-04	0.15975136 E-04
7	0.31214797 E-02	0.41080178 E-03	0.10689150 E-03	0.39117460 E-04	0.17529510 E-04	0.89860145 E-05
8	0.49943673 E-01	0.65728294 E-02	0.17102635 E-02	0.62587936 E-03	0.28047215 E-03	0.14377623 E-03

lack of relationship. It may be concluded that the higher modes are meaningless, insofar as their relationship to the real structure is concerned.

V. Results

In assessing the results of this study as embodied in Eq. (27), it is necessary to compare values of $\delta\lambda$ as given by that equation to comparable values obtained by direct eigenvalue solutions obtained for the structure of Fig. 1. As noted previously, these solutions were carried out for as many as 56 *dof*. All of the computed eigenvalues are given in Tables 3 and 4. In Fig. 3, curves are plotted for each mode shown in Table 1, comparing the eigenvalues obtained for the 56-*dof* model with those for the 16-, 24-, 32-, 40-, and 48-*dof* models. These curves show that the eigenvalues for the first 33 modes, as obtained from analysis of the 56-*dof* model, can be considered accurate. Therefore, those modes can be used as standards for comparison, insofar as eigenvalues are concerned.

Tables 5 through 8 show calculated values of $(\lambda_n^{(56)} - \lambda_n^{(r)})/\lambda_n^{(r)}$ for each mode included in Table 1, where

$\lambda_n^{(56)}$ = eigenvalue in the nth mode for the 56-*dof* model

$\lambda_n^{(r)}$ = eigenvalue in the nth mode for the rth-*dof* model

$r = 16, 24, 32,$ and 40.

These tables also include values of $\delta\lambda/\lambda_0$ where $\delta\lambda$ is obtained from Eq. (27) and λ_0 takes the values $\lambda_n^{(r)}$.

These results are plotted in Figs. 4 through 7 for the 16-, 24-, 32-, and 40-*dof* models. In each case, the eigenvalues (as compared with the 56-*dof* model) are very accurate in the lower modes and tend to become very inaccurate in the higher modes. The transition is abrupt, occurring either very suddenly at a well-defined mode number or with somewhat more gradual deterioration over two or, at most, three mode numbers. In all cases, the comparable value of $\delta\lambda/\lambda_0$ as determined from Eq. (27) shows the same abrupt deterioration at the same range of critical mode numbers.

Table 3. Eigenvalues of 16-, 24-, and 32-*dof* systems

Mode	16 *dof*	24 *dof*	32 *dof*
1	5.494	5.494	5.494
2	1.192	1.192	1.192
3	0.5777	0.5777	0.5777
4	0.4998×10^{-1}	0.4998×10^{-1}	0.4998×10^{-1}
5	0.4032×10^{-1}	0.4032×10^{-1}	0.4033×10^{-1}
6	0.1342×10^{-1}	0.1343×10^{-1}	0.1344×10^{-1}
7	0.7752×10^{-2}	0.7778×10^{-2}	0.7779×10^{-2}
8	0.5555×10^{-2}	0.6559×10^{-2}	0.6559×10^{-2}
9	0.3115×10^{-2}	0.5559×10^{-2}	0.5559×10^{-2}
10	0.1796×10^{-2}	0.3115×10^{-2}	0.3115×10^{-2}
11	0.1379×10^{-2}	0.2658×10^{-2}	0.2660×10^{-2}
12	0.7792×10^{-3}	0.1541×10^{-2}	0.1708×10^{-2}
13	0.3555×10^{-3}	0.7800×10^{-3}	0.1545×10^{-2}
14	0.2735×10^{-3}	0.7323×10^{-3}	0.7800×10^{-3}
15	0.1659×10^{-3}	0.5813×10^{-3}	0.7334×10^{-3}
16	0.6201×10^{-4}	0.4106×10^{-3}	0.5884×10^{-3}
17	—	0.3482×10^{-3}	0.5115×10^{-3}
18	—	0.2720×10^{-3}	0.4106×10^{-3}
19	—	0.1280×10^{-3}	0.3477×10^{-3}
20	—	0.1027×10^{-3}	0.1905×10^{-3}
21	—	0.7870×10^{-4}	0.1435×10^{-3}
22	—	0.5885×10^{-4}	0.1154×10^{-3}
23	—	0.2107×10^{-4}	0.1068×10^{-3}
24	—	0.1705×10^{-4}	0.1024×10^{-3}
25	—	—	0.7889×10^{-4}
26	—	—	0.6043×10^{-4}
27	—	—	0.2970×10^{-4}
28	—	—	0.2675×10^{-4}
29	—	—	0.2112×10^{-4}
30	—	—	0.1714×10^{-4}
31	—	—	0.6682×10^{-5}
32	—	—	0.4805×10^{-5}

Table 4. Eigenvalues of 40-, 48-, and 56-*dof* systems

Mode	40 *dof*	48 *dof*	56 *dof*
1	5.494	5.494	5.494
2	1.192	1.192	1.192
3	0.5777	0.5777	0.5777
4	0.4998×10^{-1}	0.4998×10^{-1}	0.4998×10^{-1}
5	0.4033×10^{-1}	0.4033×10^{-1}	0.4033×10^{-1}
6	0.1344×10^{-1}	0.1344×10^{-1}	0.1344×10^{-1}
7	0.7780×10^{-2}	0.7780×10^{-2}	0.7780×10^{-2}
8	0.6559×10^{-2}	0.6559×10^{-2}	0.6559×10^{-2}
9	0.5559×10^{-2}	0.5559×10^{-2}	0.5559×10^{-2}
10	0.3115×10^{-2}	0.3115×10^{-2}	0.3115×10^{-2}
11	0.2663×10^{-2}	0.2663×10^{-2}	0.2663×10^{-2}
12	0.1708×10^{-2}	0.1708×10^{-2}	0.1708×10^{-2}
13	0.1546×10^{-2}	0.1546×10^{-2}	0.1546×10^{-2}
14	0.7800×10^{-3}	0.7800×10^{-3}	0.7800×10^{-3}
15	0.7335×10^{-3}	0.7335×10^{-3}	0.7335×10^{-3}
16	0.6262×10^{-3}	0.6262×10^{-3}	0.6262×10^{-3}
17	0.5889×10^{-3}	0.5892×10^{-3}	0.5892×10^{-3}
18	0.5110×10^{-3}	0.5122×10^{-3}	0.5123×10^{-3}
19	0.4106×10^{-3}	0.4106×10^{-3}	0.4106×10^{-3}
20	0.3478×10^{-3}	0.3478×10^{-3}	0.3478×10^{-3}
21	0.1912×10^{-3}	0.2804×10^{-3}	0.2804×10^{-3}
22	0.1668×10^{-3}	0.1912×10^{-3}	0.1913×10^{-3}
23	0.1425×10^{-3}	0.1667×10^{-3}	0.1675×10^{-3}
24	0.1147×10^{-3}	0.1428×10^{-3}	0.1437×10^{-3}
25	0.1068×10^{-3}	0.1150×10^{-3}	0.1429×10^{-3}
26	0.1024×10^{-3}	0.1068×10^{-3}	0.1150×10^{-3}
27	0.6971×10^{-4}	0.1024×10^{-3}	0.1068×10^{-3}
28	0.6269×10^{-4}	0.7078×10^{-4}	0.1024×10^{-3}
29	0.3916×10^{-4}	0.6806×10^{-4}	0.7077×10^{-4}
30	0.3818×10^{-4}	0.6113×10^{-4}	0.6806×10^{-4}
31	0.2977×10^{-4}	0.3916×10^{-4}	0.6124×10^{-4}
32	0.2866×10^{-4}	0.3804×10^{-4}	0.3917×10^{-4}
33	0.2671×10^{-4}	0.3123×10^{-4}	0.3825×10^{-4}
34	0.1628×10^{-4}	0.2921×10^{-4}	0.3282×10^{-4}
35	0.1330×10^{-4}	0.2671×10^{-4}	0.3102×10^{-4}
36	0.9790×10^{-5}	0.1765×10^{-4}	0.2919×10^{-4}
37	0.6422×10^{-5}	0.1753×10^{-4}	0.2671×10^{-4}
38	0.5518×10^{-5}	0.1551×10^{-4}	0.1764×10^{-4}
39	0.3132×10^{-5}	0.1343×10^{-4}	0.1753×10^{-4}
40	0.1704×10^{-5}	0.1047×10^{-4}	0.1601×10^{-4}
41	—	0.9779×10^{-5}	0.1541×10^{-4}
42	—	0.6852×10^{-5}	0.1074×10^{-4}
43	—	0.4860×10^{-5}	0.9780×10^{-5}
44	—	0.4387×10^{-5}	0.8986×10^{-5}
45	—	0.3062×10^{-5}	0.7670×10^{-5}
46	—	0.1996×10^{-5}	0.6816×10^{-5}
47	—	0.1411×10^{-5}	0.6367×10^{-5}
48	—	0.7319×10^{-6}	0.4383×10^{-5}
49	—	—	0.4261×10^{-5}
50	—	—	0.3802×10^{-5}
51	—	—	0.2876×10^{-5}
52	—	—	0.2248×10^{-5}
53	—	—	0.1799×10^{-5}
54	—	—	0.1387×10^{-5}
55	—	—	0.9037×10^{-6}
56	—	—	0.4563×10^{-6}

A comparison of modal quality as indicated by differences in eigenvectors is more difficult to make. Recognizing, however, that eigenvectors have the property of uniqueness in direction, a comparison of their directions may be made. Specifically, this is done by finding a generalized angle between the eigenvectors of the 16-, 24-, and 32-*dof* models and those of the 56-*dof* model. Because this involves vectors of different dimensions, the 56-*dof* eigenvector is truncated to match the dimension of the *r dof* vector to which it is compared.

The scalar product of any two vectors, say $\mathbf{q}_1$, and $\mathbf{q}_2$, is given by $\mathbf{q}_1 \cdot \mathbf{q}_2 = q_1 q_2 \cos(q_1, q_2)$. The generalized $\cos(q_1, q_2)$ is given by

$$\cos^2(q_1, q_2) = \frac{(\mathbf{q}_1 \cdot \mathbf{q}_2)^2}{(\mathbf{q}_1 \cdot \mathbf{q}_1)(\mathbf{q}_2 \cdot \mathbf{q}_2)}$$

The generalized $\sin(q_1, q_2)$ is given by $\sin^2(\mathbf{q}_1, \mathbf{q}_2) = 1 - \cos^2(\mathbf{q}_1, \mathbf{q}_2)$. In matrix form, this equation appears as follows:

$$\sin^2 \varepsilon = 1 - \frac{(\{\mathbf{q}_0^{(r)}\}_n^T [\mathbf{m}] \{\tilde{\mathbf{q}}_0^{(56)}\}_n)^2}{(\{\mathbf{q}_0^{(r)}\}_n^T [\mathbf{m}] \{\mathbf{q}_0^{(r)}\}_n)(\{\tilde{\mathbf{q}}_0^{(56)}\}_n [m] \{\mathbf{q}_0^{(56)}\}_n)} \tag{28}$$

where

$\sin^2 \varepsilon$ = a measure of eigenvector error

$\{\mathbf{q}_0^{(r)}\}_n$ = eigenvector in nth mode for r *dof* model

$\{\tilde{\mathbf{q}}_0^{(56)}\}_n$ = truncated eigenvector in nth mode for 56-*dof* model

$[\mathbf{m}] = r \times r$ mass matrix.

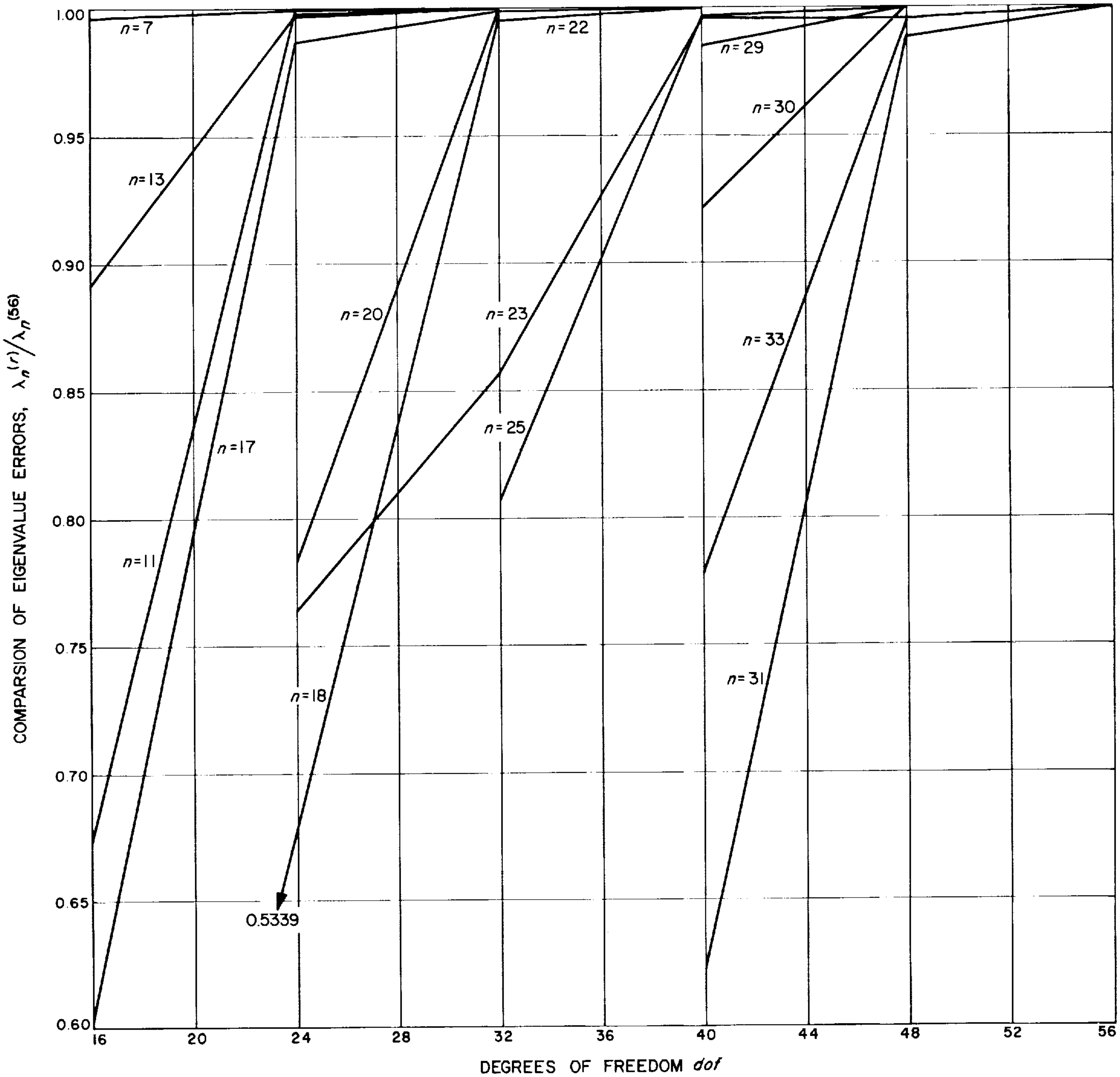

Figure 3. Eigenvalue ratios $\frac{\lambda^{(r)}}{\lambda^{(56)}}$

In Eq. (28), mass weighting is used in recognition of the standard modal orthogonality criterion. For two equal vectors it is clear that $\sin^2 \varepsilon = 0$, and that it becomes unity for two orthogonal vectors.

Equation (28) is applied to the 16-, 24-, and 32-*dof* models and the results are shown in Table 9, and are plotted in Figs. 8 through 10, together with the corresponding values of $\delta\lambda/\lambda_0$ from Eq. (27). Again, it is clear that the general deterioration of the eigenvectors occurs abruptly and at the same range of mode numbers at which the eigenvalue accuracy deteriorates.

Table 5. Comparison of eigenvalue errors, 16 *dof*

Mode	$\lambda^{(16)}$	$\lambda^{(56)}$	$\frac{\lambda^{(56)} - \lambda^{(16)}}{\lambda^{(16)}}$	$\delta\lambda$ Eq. (27)	$\frac{\delta\lambda}{\lambda_0}$
1	0.549400 E-01	0.5494 E-01	0	0.269428 E-04	0.490404 E-05
2	0.119200 E-01	0.1192 E-01	0	0.100438 E-05	0.842603 E-06
3	0.577700 E-00	0.5777 E-00	0	0.380011 E-04	0.657801 E-04
4	0.499800 E-01	0.4998 E-01	0	0.252130 E-06	0.504461 E-05
5	0.403200 E-01	0.4033 E-01	0.25 E-03	0.919051 E-05	0.227939 E-03
6	0.134200 E-01	0.1344 E-01	0.15 E-02	0.136095 E-04	0.101412 E-02
7	0.775200 E-02	0.7780 E-02	0.36 E-02	0.279403 E-04	0.360427 E-02
8	—	0.6559 E-02	—	—	—
9	0.555500 E-02	0.5559 E-02	0.72 E-03	0.238122 E-05	0.428662 E-03
10	0.311500 E-02	0.3115 E-02	0	0.406964 E-07	0.130647 E-04
11	0.179600 E-02	0.2663 E-02	0.48 E-00	0.455158 E-03	0.253429 E-00
12	—	0.1708 E-02	—	—	—
13	0.137900 E-02	0.1546 E-02	0.12 E-00	0.241134 E-03	0.174861 E-00
14	0.779200 E-03	0.7800 E-03	0.10 E-02	0.459217 E-06	0.589345 E-03
15	—	0.7335 E-03	—	—	—
16	—	0.6262 E-03	—	—	—
17	0.355500 E-03	0.5892 E-03	0.66 E-00	0.816383 E-04	0.229644 E-00
18	0.273500 E-03	0.5123 E-03	0.87 E-00	−0.121926 E-04	−0.445798 E-01

Table 6. Comparison of eigenvalue errors, 24 *dof*

Mode	$\lambda^{(24)}$	$\lambda^{(56)}$	$\frac{\lambda^{(56)} - \lambda^{(24)}}{\lambda^{(24)}}$	$\delta\lambda$ Eq. (27)	$\frac{\delta\lambda}{\lambda_0}$
1	0.5494 E-01	0.5494 E-01	0	0.399901 E-05	0.727887 E-06
2	0.1192 E-01	0.1192 E-01	0	0.161082 E-06	0.135136 E-06
3	0.5777 E-00	0.5777 E-00	0	0.656303 E-05	0.113606 E-04
4	0.4998 E-01	0.4998 E-01	0	0.161391 E-06	0.322911 E-05
5	0.4032 E-01	0.4033 E-01	0.25 E-03	0.506336 E-05	0.125579 E-03
6	0.1343 E-01	0.1344 E-01	0.74 E-03	0.219424 E-05	0.163383 E-03
7	0.7778 E-02	0.7780 E-02	0.26 E-03	0.254166 E-05	0.326776 E-03
8	0.6559 E-02	0.6559 E-02	0	0.113761 E-07	0.173442 E-05
9	0.5559 E-02	0.5559 E-02	0	0.568145 E-07	0.102203 E-04
10	0.3115 E-02	0.3115 E-02	0	0.192048 E-08	0.616527 E-06
11	0.2658 E-02	0.2663 E-02	0.19 E-02	0.482058 E-05	0.181361 E-02
12	—	0.1708 E-02	—	—	—
13	0.1541 E-02	0.1546 E-02	0.32 E-02	0.468340 E-05	0.303920 E-02
14	0.7800 E-03	0.7800 E-03	0	0.487001 E-07	0.624360 E-04
15	0.7323 E-03	0.7335 E-03	0.16 E-02	0.897047 E-06	0.122497 E-02
16	—	0.6262 E-03	—	—	—
17	0.5813 E-03	0.5892 E-03	0.14 E-01	0.433983 E-05	0.746573 E-02
18	0.3482 E-03	0.5123 E-03	0.47 E-00	0.148794 E-04	0.427322 E-01
19	0.4106 E-03	0.4106 E-03	0	0.107298 E-07	0.261319 E-04
20	0.2720 E-03	0.3478 E-03	0.28 E-00	−0.157399 E-04	−0.578673 E-01
21	—	0.2804 E-03	—	—	—
22	—	0.1913 E-03	—	—	—
23	0.1280 E-03	0.1675 E-03	0.31 E-00	0.151368 E-04	0.118256 E-00

Table 7. Comparison of eigenvalue errors, 32 *dof*

Mode	$\lambda^{(32)}$	$\lambda^{(56)}$	$\frac{\lambda^{(56)} - \lambda^{(32)}}{\lambda^{(32)}}$	$\delta\lambda$ Eq. (27)	$\frac{\delta\lambda}{\lambda_0}$
G 1	0.5494 E-01	0.5494 E-01	0	0.949275 E-06	0.172784 E-06
G 2	0.1192 E-01	0.1192 E-01	0	0.354581 E-07	0.297467 E-07
G 3	0.5777 E-00	0.5777 E-00	0	0.133152 E-05	0.230487 E-05
L 4	0.4998 E-01	0.4998 E-01	0	0.810465 E-08	0.162158 E-06
G 5	0.4033 E-01	0.4033 E-01	0	0.177090 E-06	0.439101 E-05
G 6	0.1344 E-01	0.1344 E-01	0	0.359922 E-06	0.267799 E-04
G 7	0.7779 E-02	0.7780 E-02	0.13 E-03	0.787631 E-06	0.101251 E-03
L 8	0.6559 E-02	0.6559 E-02	0	0.450979 E-08	0.687572 E-06
L 9	0.5559 E-02	0.5559 E-02	0	0.307755 E-07	0.553616 E-05
L 10	0.3115 E-02	0.3115 E-02	0	0.115138 E-08	0.369625 E-06
G 11	0.2660 E-02	0.2663 E-02	0.11 E-02	0.337669 E-05	0.126943 E-02
L 12	0.1708 E-02	0.1708 E-02	0	0.500917 E-08	0.293277 E-05
G 13	0.1545 E-02	0.1546 E-02	0.65 E-03	0.101382 E-05	0.656193 E-03
L 14	0.7800 E-03	0.7800 E-03	0	0.120385 E-07	0.154339 E-04
L 15	0.7334 E-03	0.7335 E-03	0.14 E-03	0.844317 E-07	0.115124 E-03
L 16	—	0.6262 E-03	—	—	—
G 17	0.5884 E-03	0.5892 E-03	0.14 E-02	0.798808 E-06	0.135759 E-02
G 18	0.5115 E-03	0.5123 E-03	0.16 E-02	0.762469 E-06	0.149065 E-02
L 19	0.4106 E-03	0.4106 E-03	0	0.127043 E-08	0.309408 E-05
G 20	0.3477 E-03	0.3478 E-03	0.29 E-03	0.129405 E-06	0.372175 E-03
21	—	0.2804 E-03	—	—	—
L 22	0.1905 E-03	0.1913 E-03	0.42 E-02	0.285106 E-06	0.149662 E-02
G 23	0.1435 E-03	0.1675 E-03	0.17 E-00	0.838132 E-06	0.584064 E-02
24	—	0.1437 E-03	—	—	—
G 25	0.1154 E-03	0.1429 E-03	0.24 E-00	0.662037 E-05	0.573689 E-01
G 26	—	0.1150 E-03	—	—	—
L 27	0.1068 E-03	0.1068 E-03	0	0.632306 E-06	0.592047 E-02
L 28	0.1024 E-03	0.1024 E-03	0	−0.704725 E-06	−0.688208 E-02

Table 8. Comparison of eigenvalue errors, 40 *dof*

Mode	$\lambda^{(40)}$	$\lambda^{(56)}$	$\frac{\lambda^{(56)} - \lambda^{(40)}}{\lambda^{(40)}}$	$\delta\lambda$ Eq. (27)	$\frac{\delta\lambda}{\lambda_0}$
G 1	0.5494 E-01	0.5494 E-01	0	0.276419 E-06	0.503128 E-07
G 2	0.1192 E-01	0.1192 E-01	0	0.109938 E-07	0.922295 E-08
G 3	0.5777 E-00	0.5777 E-00	0	0.441925 E-06	0.764973 E-06
L 4	0.4998 E-01	0.4998 E-01	0	0.456692 E-08	0.913749 E-07
G 5	0.4033 E-01	0.4033 E-01	0	0.119516 E-06	0.296346 E-05
G 6	0.1344 E-01	0.1344 E-01	0	0.113099 E-06	0.841513 E-05
G 7	0.7780 E-02	0.7780 E-02	0	0.171393 E-06	0.220299 E-04
L 8	0.6559 E-02	0.6559 E-02	0	0.732608 E-09	0.111695 E-06
L 9	0.5559 E-02	0.5559 E-02	0	0.303569 E-08	0.546086 E-06
L 10	0.3115 E-02	0.3115 E-02	0	0.128100 E-09	0.411235 E-07
G 11	0.2663 E-02	0.2663 E-02	0	0.176879 E-06	0.664211 E-04
L 12	0.1708 E-02	0.1708 E-02	0	0.827043 E-09	0.484217 E-06
G 13	0.1546 E-02	0.1546 E-02	0	0.352864 E-06	0.228243 E-03
L 14	0.7800 E-03	0.7800 E-03	0	0.359134 E-08	0.460428 E-05
L 15	0.7335 E-03	0.7335 E-03	0	0.313258 E-07	0.427072 E-04
L 16	0.6262 E-03	0.6262 E-03	0	0.108750 E-07	0.173667 E-04
G 17	0.5889 E-03	0.5892 E-03	0.51 E-03	0.334345 E-06	0.567745 E-03
G 18	0.5110 E-03	0.5123 E-03	0.25 E-02	0.127575 E-05	0.249657 E-02
L 19	0.4106 E-03	0.4106 E-03	0	0.356042 E-09	0.867125 E-06
G 20	0.3478 E-03	0.3478 E-03	0	0.455064 E-07	0.130841 E-03
L 21	—	0.2804 E-03	—	—	—
L 22	0.1912 E-03	0.1913 E-03	0.52 E-03	0.414331 E-07	0.216700 E-03
G 23	0.1668 E-03	0.1675 E-03	0.42 E-02	0.774400 E-06	0.464269 E-02
L 24	—	0.1437 E-03	—	—	—
G 25	0.1425 E-03	0.1429 E-03	0.28 E-02	0.363620 E-06	0.255172 E-02
G 26	0.1147 E-03	0.1150 E-03	0.26 E-02	0.353712 E-06	0.308380 E-02
L 27	0.1068 E-03	0.1068 E-03	0	0.231789 E-08	0.217031 E-04
L 28	0.1024 E-03	0.1024 E-03	0	0.504278 E-08	0.492459 E-04
G 29	0.6971 E-04	0.7077 E-04	0.15 E-01	0.151212 E-06	0.216915 E-02
L 30	0.6269 E-04	0.6806 E-04	0.86 E-01	0.120752 E-05	0.192617 E-01
G 31	0.3818 E-04	0.6124 E-04	0.60 E-00	−0.151980 E-05	−0.398062 E-01
L 32	0.3916 E-04	0.3917 E-04	0.26 E-03	−0.772811 E-07	−0.197347 E-02
G 33	0.2977 E-04	0.3825 E-04	0.28 E-00	−0.954271 E-05	−0.320548 E-00

Table 9. Eigenvector errors, $\sin^2 \varepsilon$ from Eq. (28)

Mode	16 *dof*	24 *dof*	32 *dof*	Mode	16 *dof*	24 *dof*	32 *dof*
1	0.000000	0.000000	0.000000	15	—	0.000118	0.000000
2	0.000000	0.000000	0.000000	16	—	—	—
3	0.000000	0.000000	0.000000	17	0.030021	0.035630	0.000008
4	0.000000	0.000000	0.000000	18	0.052096	1.144723	0.000019
5	0.000000	0.000000	0.000000	19	—	−0.000001	0.000000
6	0.000005	0.000000	0.000000	20	—	1.178584	0.028150
7	0.000067	0.000000	0.000000	21	—	—	—
8	—	0.000000	0.000000	22	—	—	0.148993
9	0.000045	0.000000	0.000000	23	—	1.556600	2.349014
10	0.000124	0.000000	0.000000	24	—	—	—
11	0.008298	0.000002	0.000000	25	—	—	−14.855941
12	—	—	0.000000	26	—	—	—
13	1.007877	0.000515	−0.000116	27	—	—	0.000082
14	0.085626	0.005203	−0.000003	28	—	—	0.000590

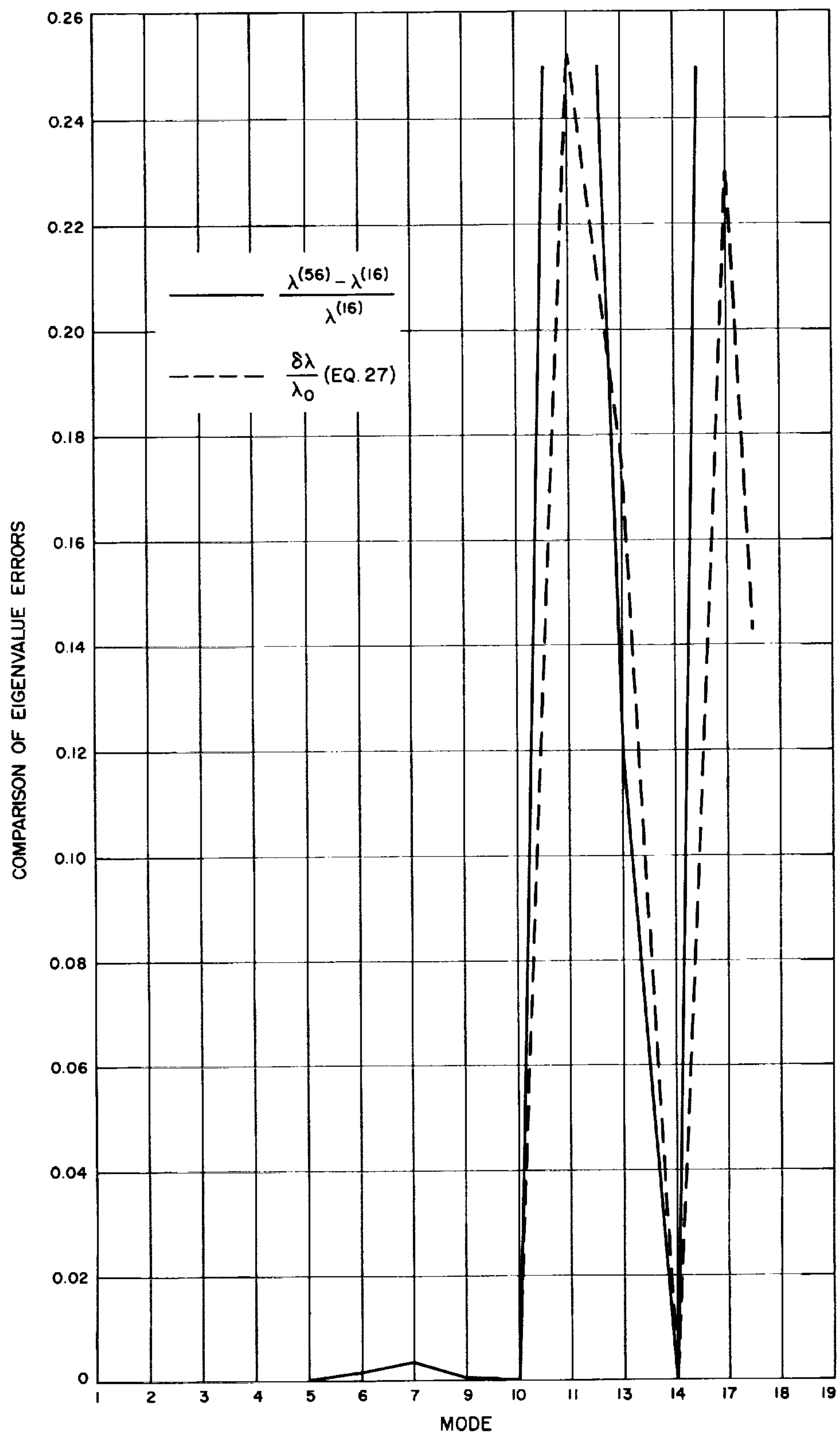

Figure 4. Mode vs $\frac{\delta\lambda}{\lambda_0}$ and $\frac{\lambda^{(56)} - \lambda^{(r)}}{\lambda^{(r)}}$, 16-*dof* system

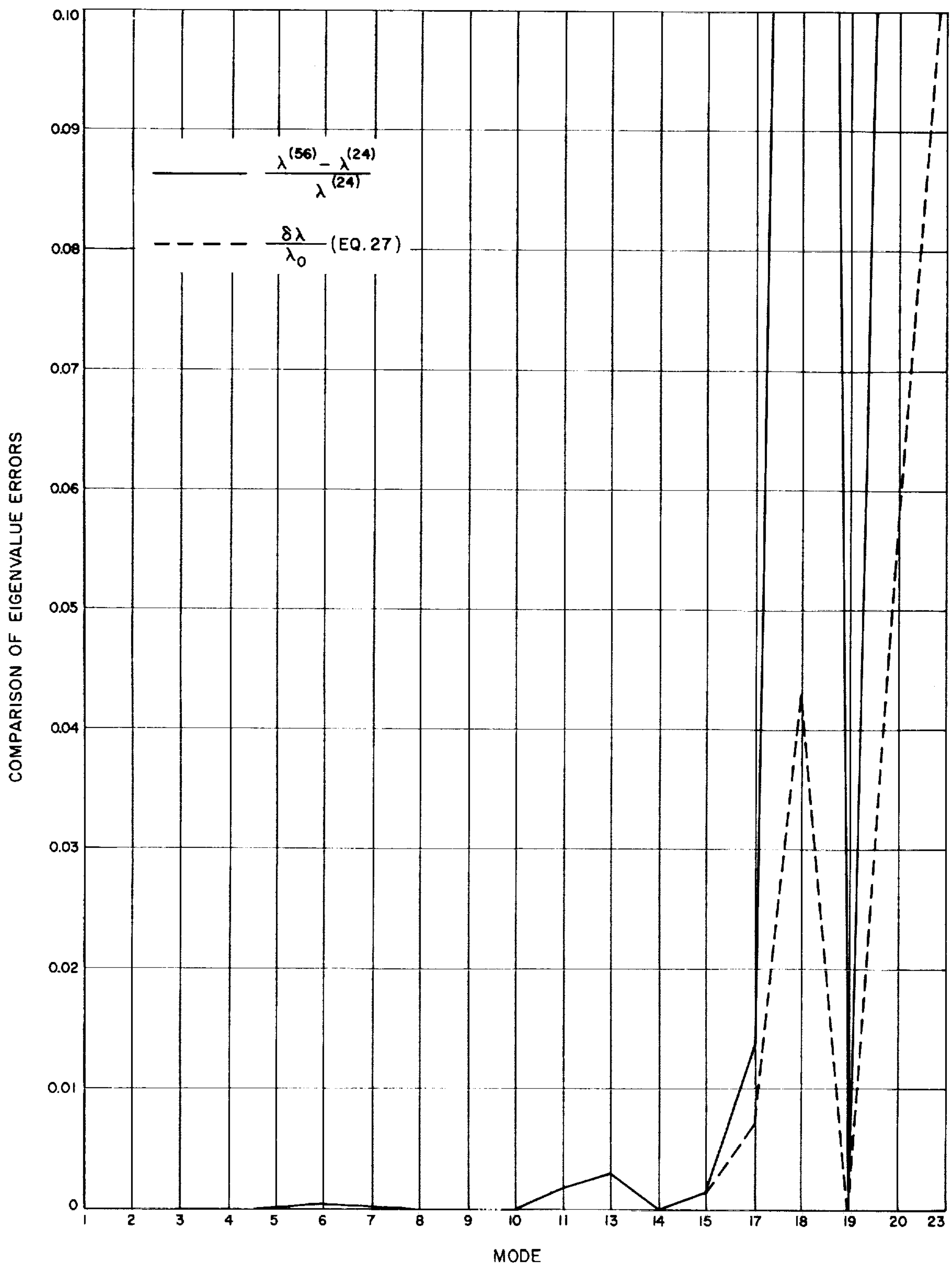

Figure 5. Mode vs $\frac{\delta\lambda}{\lambda_0}$ and $\frac{\lambda^{(56)} - \lambda^{(r)}}{\lambda^{(r)}}$, 24-dof system

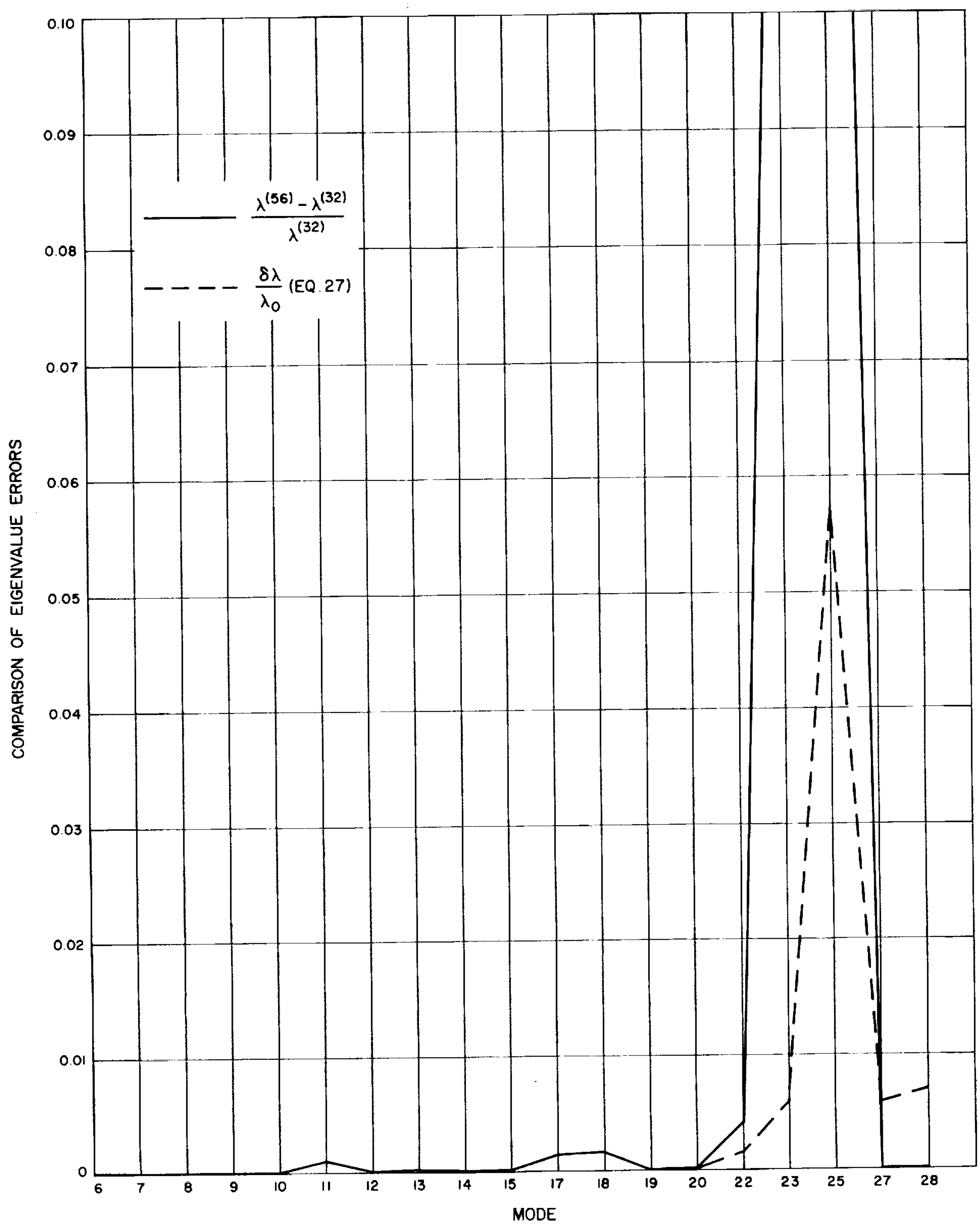

Figure 6. Mode vs $\frac{\lambda\delta}{\lambda_0}$ and $\frac{\lambda^{(56)} - \lambda^{(r)}}{\lambda^{(r)}}$, 32-dof system

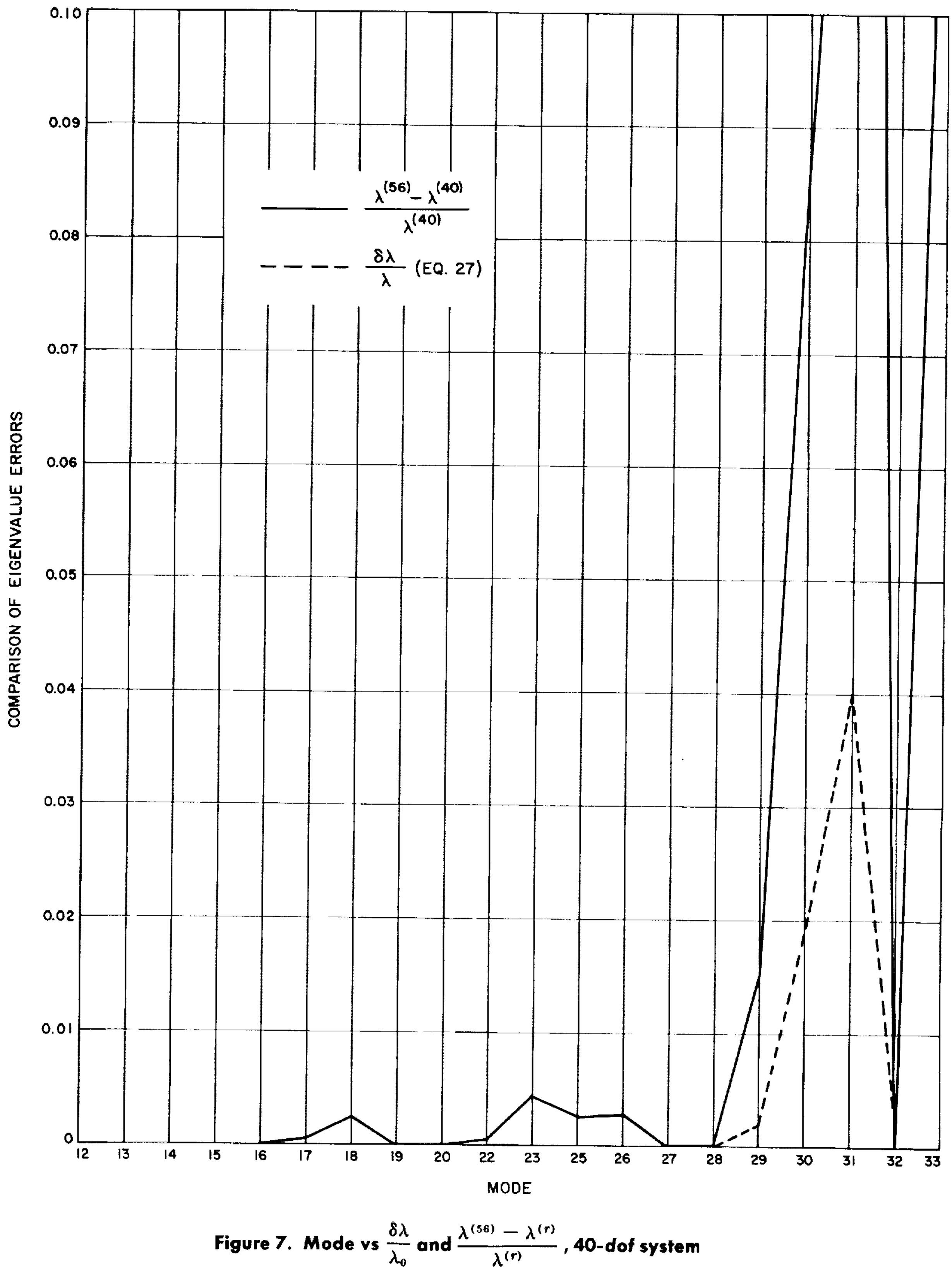

Figure 7. Mode vs $\frac{\delta\lambda}{\lambda_0}$ and $\frac{\lambda^{(56)} - \lambda^{(r)}}{\lambda^{(r)}}$, 40-dof system

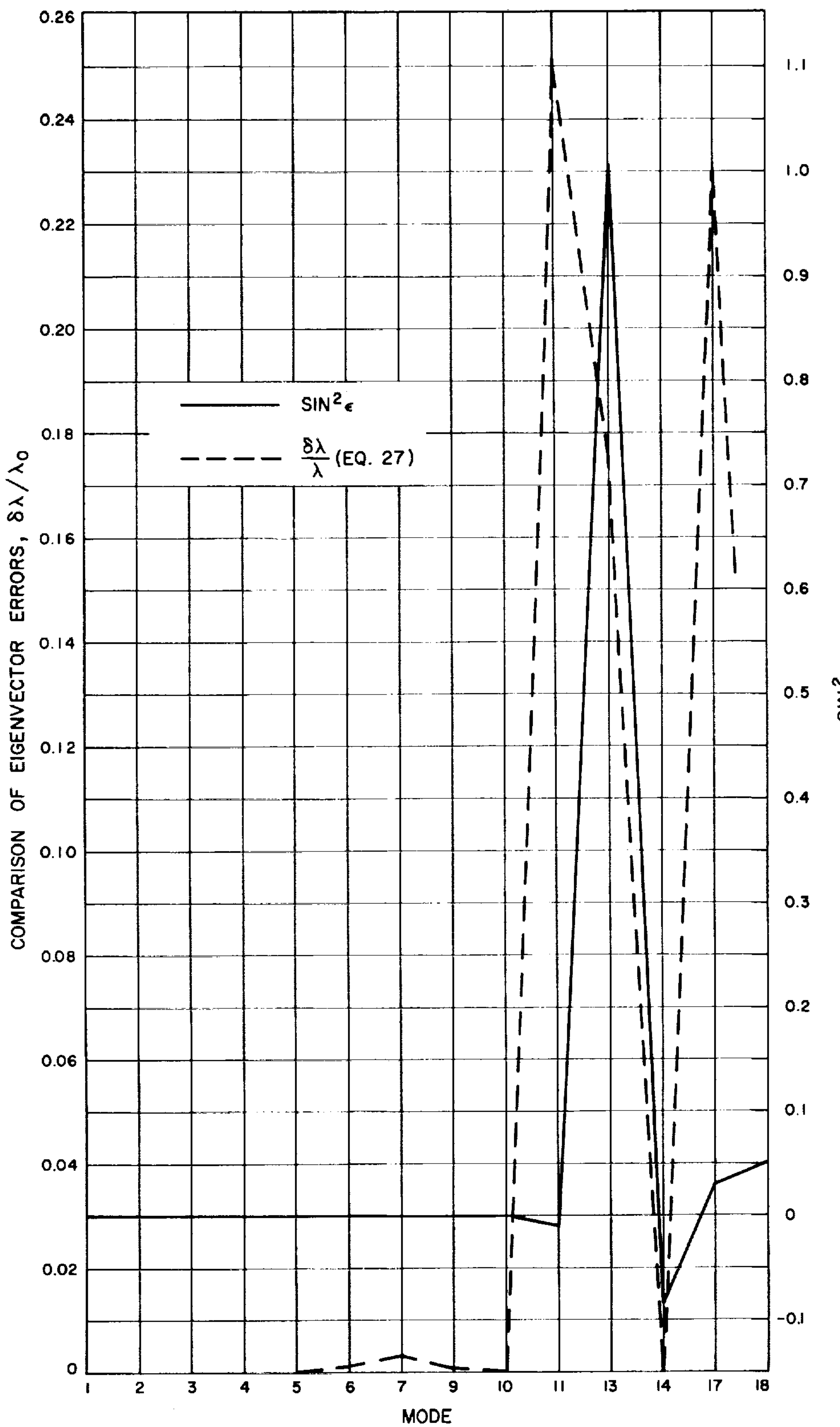

Figure 8. Sin² ε vs mode, 16-*dof* system

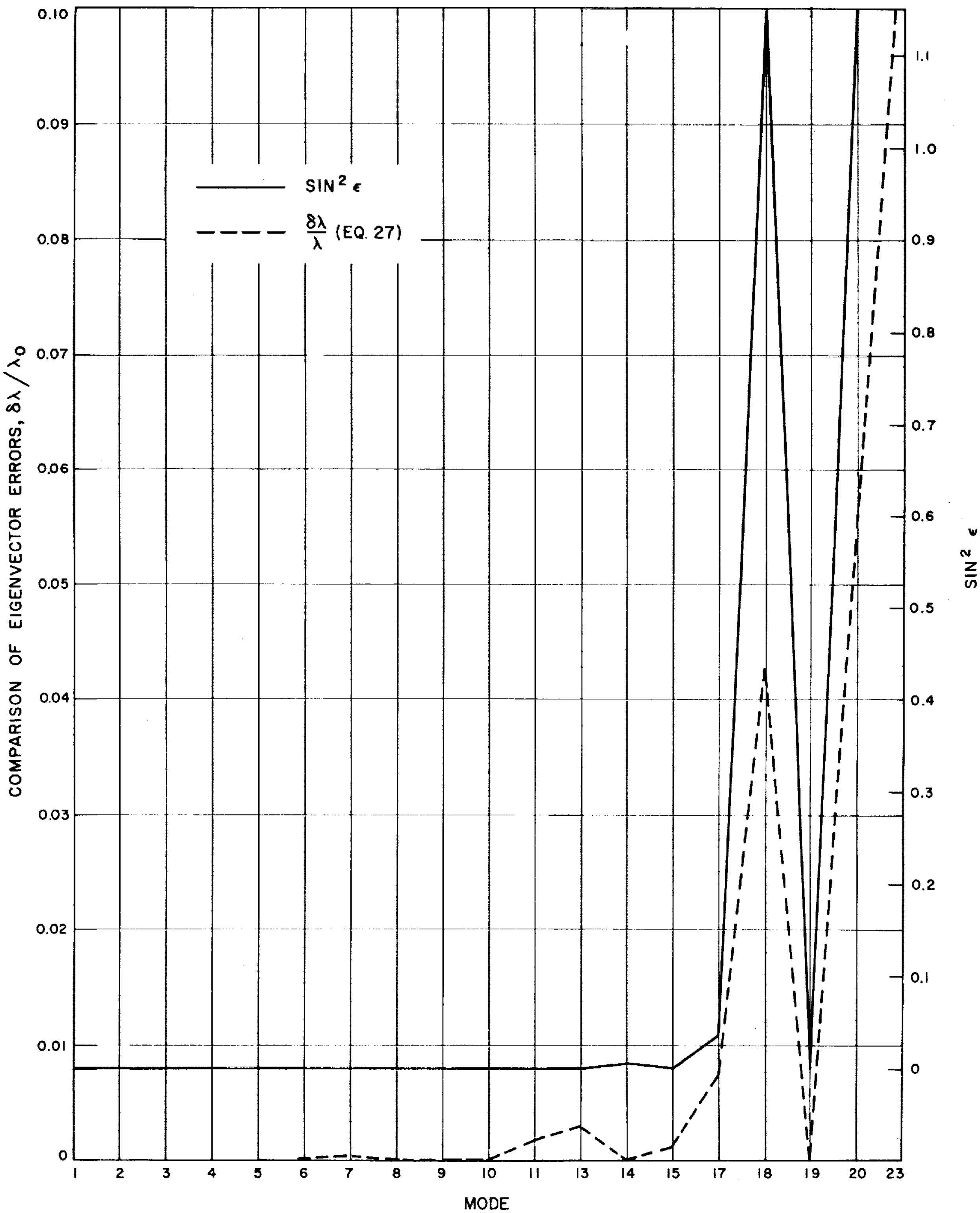

Figure 9. Sin² ε vs mode, 24-dof system

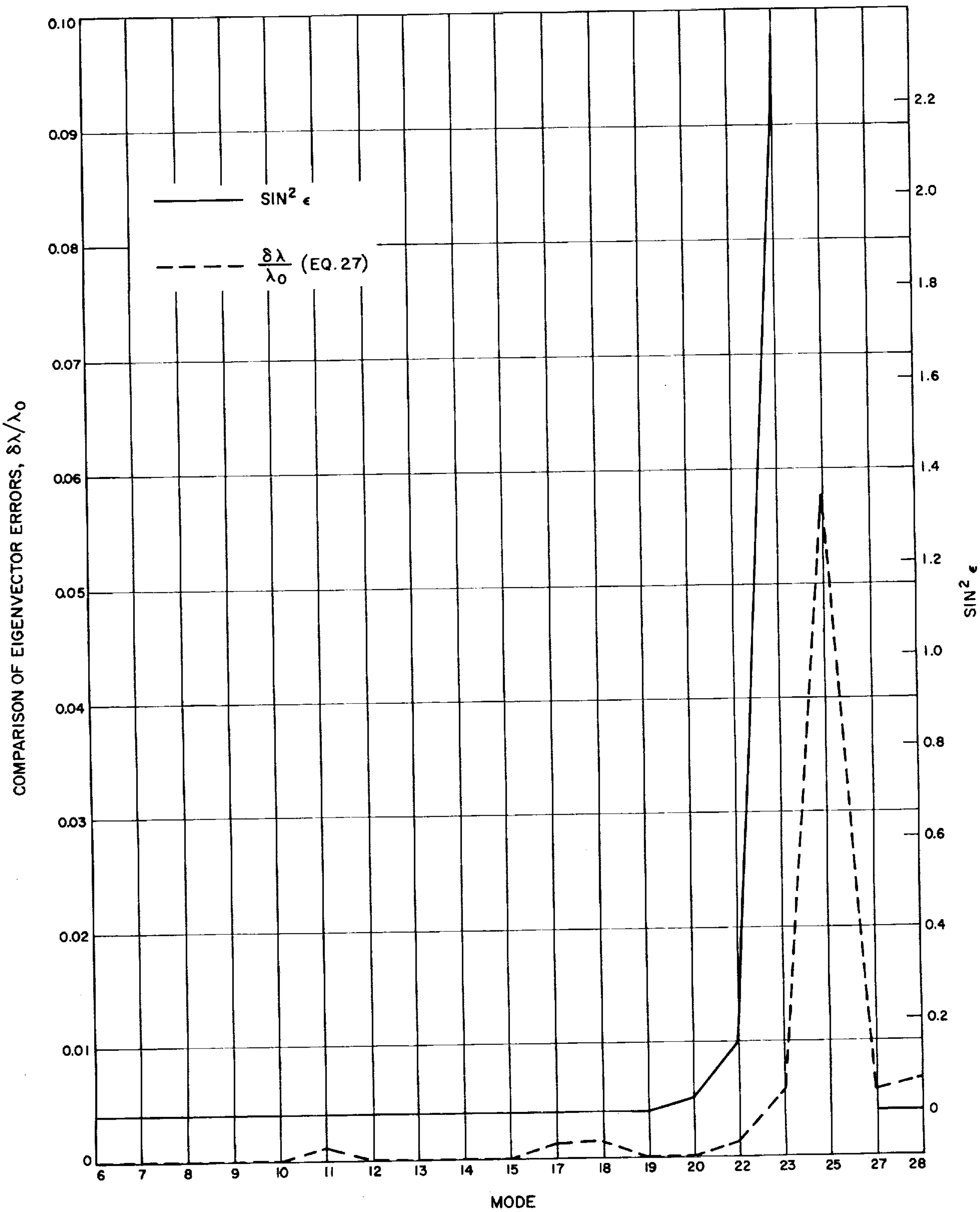

Figure 10. $\sin^2 \varepsilon$ **vs mode, 32-dof system**

VI. Conclusion

From the results of the example included in this report, it is tentatively concluded that Eq. (27) offers a valid engineering criterion for delineating between accurate and inaccurate natural modes of a structure as determined by the method of component mode synthesis. Although Eq. (27) supplies a number related only to eigenvalue error, the results show that this number serves equally well in relating to errors in the eigenvectors. Both the eigenvalues and eigenvectors deteriorate in accuracy very rapidly and at the same critical region in the natural mode spectrum.

References

1. Hurty, W. C., *Dynamic Analysis of Structural Systems by Component Mode Synthesis*, Technical Report 32-350. Jet Propulsion Laboratory, Pasadena, Calif., Jan. 15, 1964.

2. Hurty, W. C., "Dynamic Analysis of Structural Systems Using Component Modes," *AIAA J.*, Vol. 3, No. 4, pp. 678–685, April, 1965.